Korean Journal of Polar Research 10(2): 67-75

Geochemistry of the Core Sediments in Maxwell Bay of the South Shetland Islands, West Antarctica

Dongseon Kim, Byong-Kwon Park, Ho Il Yoon, and Dong Yup Kim

Polar Research Center, Korea Ocean Research & Development Institute, Ansan P.O. Box 29, Seoul 425-600, Korea

ABSTRACT. Downcore distributions of major, minor, and rare earth elements (REEs) were determined to investigate the major factors influencing their concentrations in Maxwell Bay core sediments. Sediment grain size is the primary factor constraining the concentrations of Ti, Cr, Na, and K at core A1, and Na, Mg, Zn, Cr, Ni, and K at core A2. At both cores, meanwhile, Fe, Co, and Cu concentrations are closely associated with sulfide minerals. The Ce and Eu anomalies and shale-normalized REE patterns indicate that the Maxwell Bay sediments are significantly influenced by the hydrothermal system, and oxidizing conditions have been maintained during the entire sediment deposition.

Key Words: Major, minor, rare earth elements, core sediments, Maxwell Bay

Introduction

The chemical compositions of marine sediments reflect the extent of chemical, oceanographic and sedimentary controls on their supply to, distribution in and removal from the ocean. There are many mechanisms that influence the concentrations of major, minor, and rare earth elements (REEs) in marine sediments, including the chemical composition of sedimentary detritus delivered to the ocean, the partitioning of individual elements between solid and solution phases, the biogeochemical cycle of the elements in the ocean, and the diagenetic element recycling in bottom sediments (Francois 1988; Pruysers *et al.* 1991; Calvert and Pederson 1993). Many minor elements have multiple valency states at Earth surface conditions and typically have different solubility in oxygenated or oxygen deficient seawater. These elements are also partitioned between the solid and solution phases to different extents under different redox conditions (Dyrssen and Kremling 1990). Therefore, examination of the chemical behavior of the minor elements in the sediment column could potentially provide valuable information on the chemical state of the environment of deposition of ancient sediments (Piper and Issacs 1996). The chemistry of the REEs, especially their similar chemical properties and low solubility that allow only limited elemental fractionation during weathering and diagenesis, makes these elements useful as geochemical indicators in sediment and in sedimentary rocks (Fleet 1984; McLennan 1989).

Maxwell Bay is a deep and glacially influenced U-shaped fjord bounded by King George Island on the northeast and by Nelson Islands on the southwest in the South Shetland Islands, Antarctica (Fig. 1). This region belongs to a temperate to subpolar setting with warm and humid weather. Sedimentary processes in the Maxwell Bay are significantly influenced by glacial activities, and glaciomarine sediments are widely distributed in the bottom of the Maxwell Bay. The sediment column of the Maxwell Bay is clearly distinguished by several sediment layers with different sediment texture and properties

*corresponding author (dkim@kordi.re.kr)

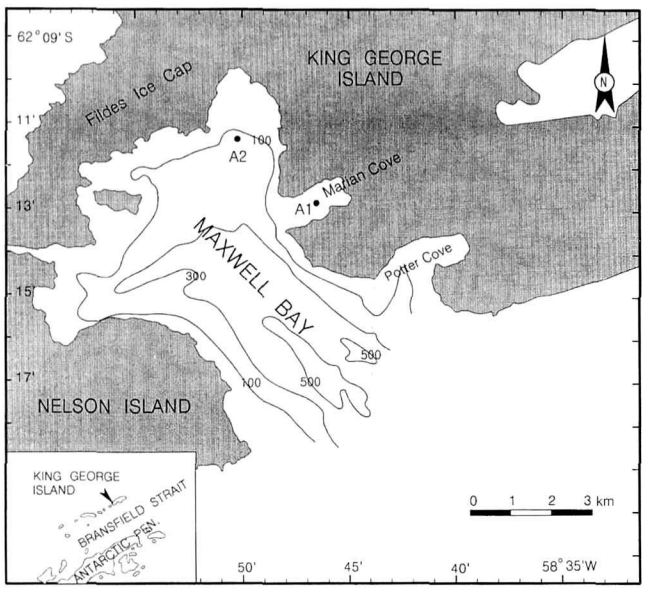

Fig. 1. Map of the study area. Solid circles indicate sediment core sites. Contours are in meters.

(Yoon *et al.* 1997). The goals of this study are to investigate downcore distributions of major, minor, and REE concentrations in the Maxwell Bay sediments and to determine major factors controlling their downcore distributions. We also elucidate the sedimentary conditions of Maxwell Bay on the basis of REE geochemistry.

Materials and Methods

Sediment cores A1 and A2 were collected with a gravity corer at a water depth of 110 m from the Maxwell Bay of the South Shetland Islands, West Antarctica (Fig. 1). Sediment subsampling was made at 5 cm intervals, and each such sample was dried at 80°C for 4 days and then ground. Sediment grain size analysis was conducted by the Sedigraph after removing organic matter and calcium carbonate. Total organic carbon (TOC) contents were determined by a Carlo-Erba CNS analyzer after eliminating inorganic carbon by 10% HCl. Total carbon and sulfur contents were also analyzed by the Carlo-Erba CNS analyzer. Calcium carbonate contents were calculated by subtracting TOC contents from total carbon contents. Major and minor elements were measured by the Inductively Coupled Plasma - Atomic Emission Spectrometry (ICP-AES) at the Korea Basic Science Center. Rare earth element concentrations were determined by the Inductively Coupled Plasma - Mass Spectrometry (ICP-MS) at the Korea Basic Science Center. Complete sample dissolution prior to introduction into the ICP-AES and ICP-MS was achieved by HNO_3-HF-$HClO_4$ total digestion in Teflon beaker (Park and Yoon 1994).

RESULTS AND DISCUSSION

Major elements

Downcore variations of major elements are shown in Figure 2. Sodium and Mg concentrations generally decrease with increasing core depth at cores A1 and A2, whereas Ca and Fe concentrations increase at both cores. Potassium, Al and Ti concentrations decrease with core depth at core A1, but they do not show a significant change at core A2. Manganese does not display any distinct downcore trend with small fluctuation at both cores.

The upper sediments (top 100 cm) are mostly composed of silty clay at core A1 and A2, but silty sand is dominant in the lower sediments (Fig. 3a). Total organic carbon contents decrease rapidly with increasing core depth at both cores (Fig. 3b), meanwhile $CaCO_3$ and total sulfur (TS) contents increase with core depth (Figs. 3c and 3d). Especially, TS contents increase abruptly at the 100 - 120 cm core depth of both cores.

In general, Al and Ti are incorporated in detrital components of marine sediments which consist of rock fragments and minerals derived from the continents by weathering (Calvert 1976). Thus their concentrations are generally controlled by sediment texture; high concentrations are observed in fine grain sediments. At core A1, Al and Ti concentrations decrease slightly with core depth, which is likely due to the increase of sediment grain size with core depth. At core A2, however, Al and Ti show nearly constant concentrations with core depth, in spite of a large increase of sediment grain size. It implies that Al and Ti concentrations are not related to sediment texture at core A2. Potassium concentration is

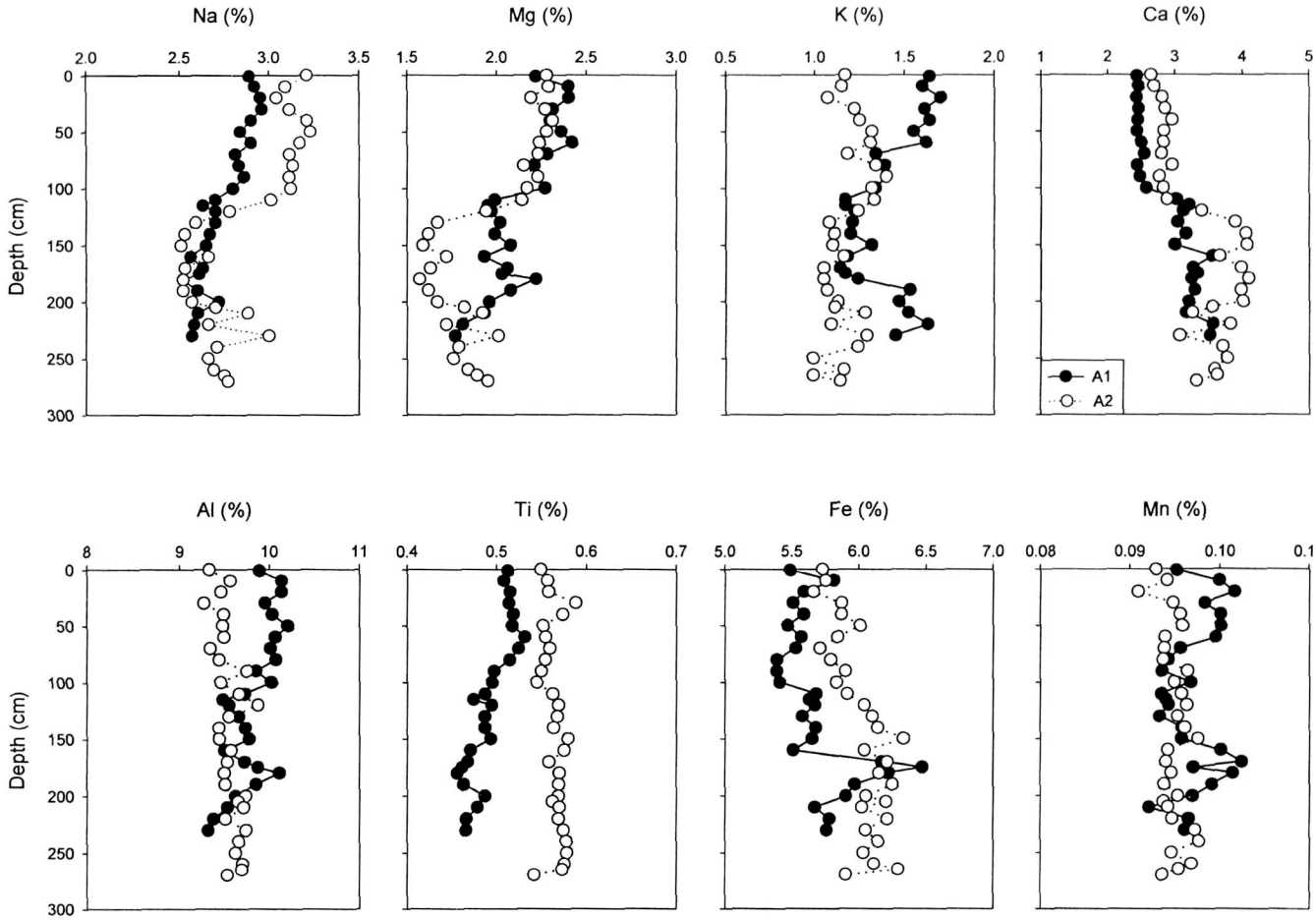

Fig. 2. Downcore variations of major element concentrations at cores A1 and A2. Filled circle indicates core A1, and open one core A2.

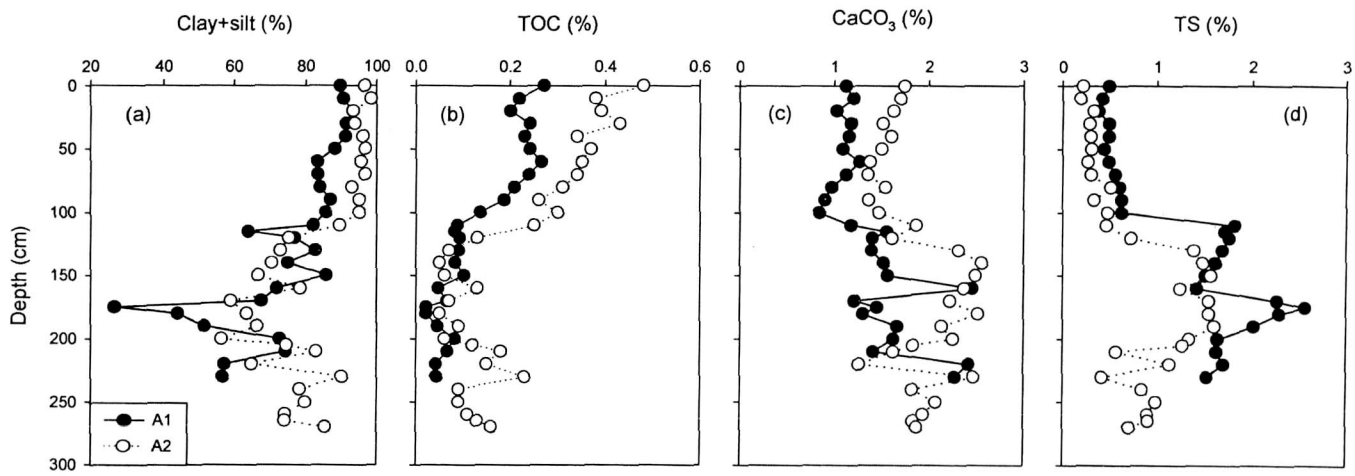

Fig. 3. Downcore variations of (a) clay+silt, (b) TOC, (c) $CaCO_3$, and (d) TS contents at cores A1 and A2. Filled circle represents core A1, and open one core A2.

also almost constant at core A2, while it decreases with core depth at core A1. Therefore, mineral composition of core A1 sediments is rather different from that of core A2 sediments. It is likely that K-feldspar is more enriched in coarser-grained material at core A2 than at core A1, which results in the almost constant concentrations of Al, Ti, and K with core depth, in spite of large changes of sediment

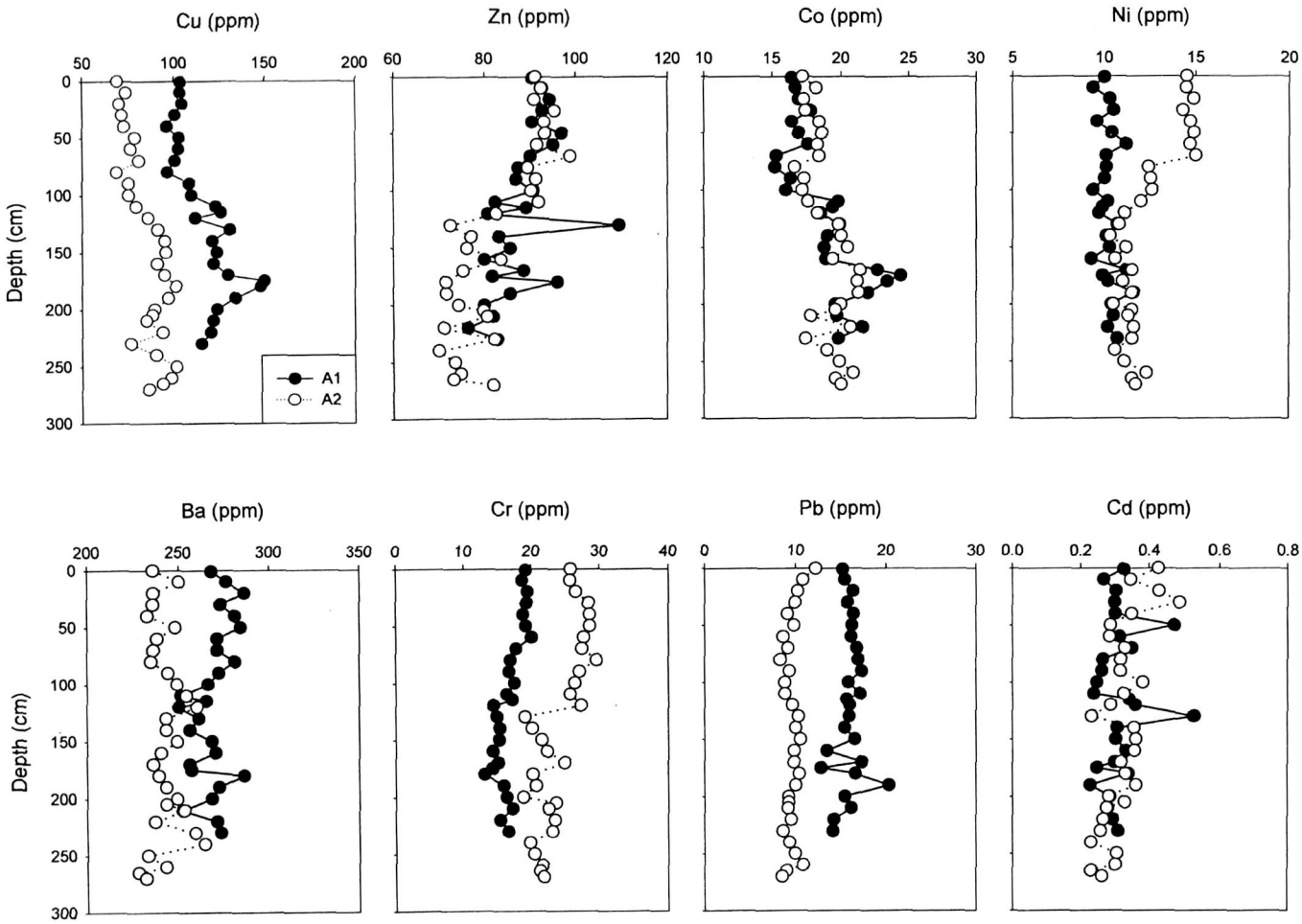

Fig. 4. Downcore variations of minor element concentrations at cores A1 and A2. Filled circle indicates core A1, and open one core A2.

grain size at core A2.

Downcore variations of Na and Mg are rather similar to that of clay and silt contents at cores A1 and A2 (Figs. 2 and 3a), which reflects that the behavior of Na and Mg at the Maxwell Bay sediments is constrained by sediment grain size. Calcium concentration increases slightly with core depth at both cores, which results from the increase of $CaCO_3$ (Fig. 3c). Depth profile of Fe is quite similar to that of TS at both cores (Figs. 2 and 3d), suggesting that Fe concentration is controlled mainly by sulfide minerals, such as pyrite.

Minor elements

Minor elements show different downcore distribution patterns at cores A1 and A2 (Fig. 4). Cu and Co concentrations increase with increasing core depth at both cores, whereas Zn and Cr exhibit a downcore decreasing trend. Ni concentration decreases with core depth at core A2, but it is almost constant at core A1. Ba, Pb, and Cd concentrations display small variations with core depth without any distinct downcore trend.

In general, many minor elements, especially Cu, Zn, Co, Cd, and Pd are well associated with sulfide minerals (Oudin 1985; Hannington *et al.* 1991). At cores A1 and A2, therefore, the downcore increase in Cu and Co concentrations is attributed to the formation of sulfide minerals in the lower part of cores A1 and A2. However, downcore profiles of Zn, Pb, Cd are somewhat different from that of TS, implying that these minor elements are not associated in sulfide minerals formed in the Maxwell Bay sediments. The downcore profiles of Zn and Cr are rather similar to that of clay and silt at both cores. Hence Zn and Cr concentrations appear to be significantly affected by the sediment grain size.

The SPSS (v. 7.1) factor-analysis programme was

Table 1. Factor loadings for five factors for the geochemical data of core A1

Factor	1	2	3	4	5
Clay+silt	0.858	0.256	–0.114	0.172	0.011
Ti	0.852	0.395	0.112	0.111	–0.009
TOC	0.835	0.418	0.235	0.092	0.015
Cr	0.819	0.184	0.319	–0.058	0.166
Na	0.792	0.483	0.225	0.001	–0.010
K	0.629	–0.114	0.584	–0.187	0.253
Cu	–0.952	–0.100	–0.108	0.045	0.058
Co	–0.919	–0.235	0.062	–0.045	0.174
TS	–0.915	–0.249	–0.265	–0.046	0.104
Fe	–0.872	0.044	0.242	–0.203	0.066
Ca	–0.742	–0.636	–0.168	–0.056	–0.013
Al	0.260	0.817	0.460	0.049	0.022
Mg	0.463	0.738	0.455	0.086	0.034
$CaCO_3$	–0.323	–0.898	0.105	–0.022	–0.130
Mn	–0.180	0.187	0.840	0.016	0.017
Ba	0.289	0.123	0.785	0.140	–0.023
Cd	0.068	–0.096	–0.016	0.963	–0.036
Zn	0.173	0.489	0.229	0.743	0.185
Ni	–0.181	–0.122	0.125	0.111	0.914
Pb	0.071	0.423	–0.094	–0.067	0.764
Variance (%)	53.3	13.3	8.7	7.5	6.8

Table 2. Factor loadings for three factors for the geochemical data of core A2

Factor	1	2	3
Na	0.981	–0.085	–0.025
Mg	0.976	–0.109	0.003
Clay+silt	0.941	–0.077	0.014
Zn	0.927	–0.172	0.104
TOC	0.926	–0.247	0.225
Cr	0.854	–0.186	–0.012
Ni	0.795	–0.365	0.264
K	0.749	0.409	–0.302
Ca	–0.981	0.090	0.017
TS	–0.954	–0.006	0.058
Cu	–0.938	0.086	–0.030
Co	–0.900	–0.133	0.051
Fe	–0.841	0.289	–0.078
$CaCO_3$	–0.706	0.220	0.256
Ba	0.064	0.868	–0.076
Mn	–0.182	0.835	–0.078
Al	–0.232	0.592	–0.514
Pb	–0.172	–0.045	0.821
Cd	0.340	–0.292	0.740
Ti	–0.433	0.423	0.443
Variance (%)	59.8	14.6	7.1

used to evaluate complex interrelationships between eight major elements, eight minor elements, clay and silt, $CaCO_3$, TS, and TOC contents. At core A1, the first five factors, using varimax rotation and based on eigen values exceeding 1.0, explain 89.5 % of the total variance in the data set (Table 1). Factor 1, accounting for 53.3 % of the data variance, show strong positive loading for clay and silt, Ti, TOC, Cr, Na, and K. Copper, Co, TS, Fe and Ca are negatively loaded on this factor. Therefore, this factor represents both the fine fraction of the sediments and sulfide minerals. The strong negative correlation between the fine fraction of the sediments and sulfide minerals indicates that sulfide minerals are significantly enriched in the coarse fraction of the sediments. Factor 2 accounts for 13.3% of the data variance and show strong positive loading of Al and Mg and negative loading of Ca and $CaCO_3$. This factor may represent carbonate factor, but the strong positive loading of Al and Mg cannot be explained by carbonate factor. Factor 3 accounts for 8.7% of the data variance and show strong positive loading of Mn and Ba. Factor 4 accounts for 7.5% of the data variance and show strong positive loading of Cd and Zn. Factor 5 accounts for 6.8% of the data variance and show strong positive loading of Ni and Pb. Except for factor 1, it is hardly explained what other 4 factors represent at core A1.

At core A2, the first three factors, using varimax rotation and based on eigen values exceeding 1.0, explain 81.5% of the total variance (Table 2). Factor 1 accounts for 59.8 % of the data variance and show strong positive loading for Na, Mg, clay and silt, Zn, TOC, Cr, Ni, and K. Calcium, TS, Cu, Co, Fe and $CaCO_3$ are negatively loaded on this factor. This factor represents the fine fraction of the sediments, sulfide minerals and $CaCO_3$. The strong negative correlation between the fine fraction of the sediments, sulfide minerals and $CaCO_3$ indicates that sulfide minerals and $CaCO_3$ are significantly enriched in the coarse fraction of the sediments. Factor 2 accounts for 14.6% of the data variance and show strong positive loading of Ba, Mn, and Al. Factor 3 accounts for 7.1% of the data variance and show

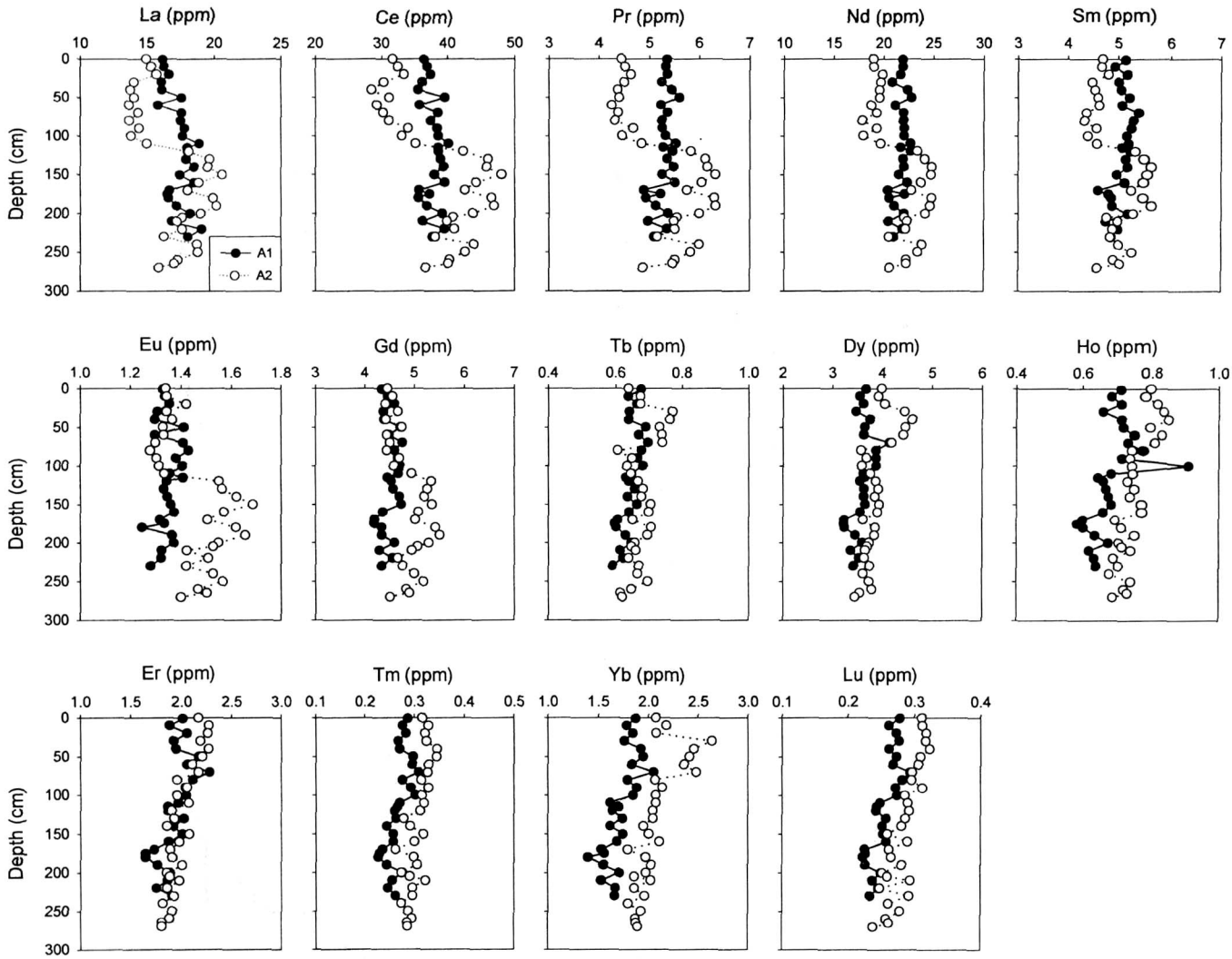

Fig. 5. Downcore variations of REE concentrations at cores A1 and A2. Filled circle represents core A1, and open one core A2.

strong positive loading of Pb, Cd, and Ti. It is difficult to explain what factors 2 and 3 represents at core A2. Consequently, sediment texture, sulfide mineral, and $CaCO_3$ factors can explain 53 and 60% of behaviors of major and minor elements at cores A1 and A2, respectively.

Rare earth elements

Downcore variations of rare earth elements (REEs) are shown in Figure 5. At core A2, La, Ce, Pr, Nd, Sm, Eu, and Gd show relatively high concentrations below 100 cm sediment depth where TS content increases rapidly with core depth (Fig. 3d). Thus, these LREEs are associated with sulfide minerals. At core A1, however, these REEs concentrations do not vary considerably with core depth, even though TS content shows a large increase below 100 cm. Terbium and Dy concentrations exhibit a small variation with core depth without any distinct downcore trend at both cores. Holmium, Er, Tm, Yb, and Lu concentrations decrease slightly with core depth at both cores, implying that these heavy rare earth elements (HREEs) are influenced by sediment texture.

The $La_n/Yb_n\{(La_{sample}/La_{NASC})/(Yb_{sample}/Yb_{NASC})\}$, which defines relative behavior of LREEs to HREEs ranges from 0.81 to 1.14 and from 0.51 to 1.01 at cores A1 and A2, respectively (Fig. 6a). The La_n/Yb_n values are much lower than 1.0 at the top 100 cm at both cores, especially at core A2 and then increase rapidly to about 1.0 at the boundary of 100 cm sediment depth. Thus LREEs are fairly depleted at the top 100 cm compared to HREEs. In seawater, LREEs are significantly depleted relative to HREEs, because

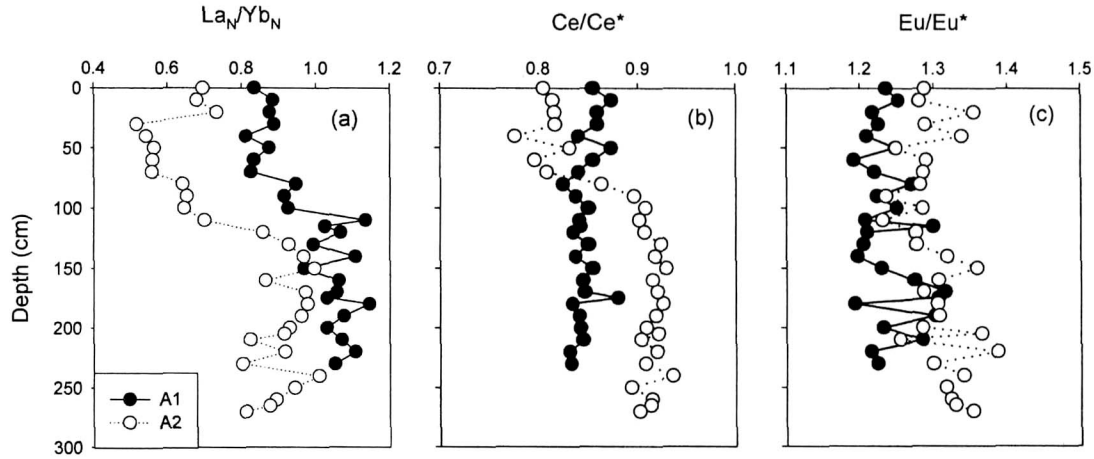

Fig. 6. Downcore variations of (a) La_n/Yb_n, (b) Ce/Ce*, and (c) Eu/Eu* at cores A1 and A2. Filled circle indicates core A1, and open one core A2.

of the relatively greater stability of HREE complexes in seawater (Brookins 1989). Hence the REE compositions at the top 100 cm may be more influenced by seawater than those below 100 cm.

The Ce anomaly (Ce/Ce*), which indicates the degree of Ce enrichment or depletion with respect to adjacent REE ranges from 0.82 to 0.88 and from 0.78 to 0.94 at cores A1 and A2, respectively (Fig. 6b). The Ce/Ce* >0.9, <1.1, and 0.9-1.1 indicates negative, positive, and no anomaly, respectively. Ce^{3+} is oxidized in the oceans to Ce^{4+} which is highly insoluble under oxidizing conditions and is preferentially incorporated or adsorbed in octahedral sites of precipitates or as CeO_2 on the surfaces of grains in bottom sediments (Elderfield and Greaves 1982; Koeppenkastrop and De Carlo 1992). Thus the Ce anomaly has been used to identify the redox conditions in ancient environments; the Ce/Ce* values are negative under oxidizing conditions (Grandjean *et al.* 1988; Liu and Schmitt 1990). At core A1, the Ce/Ce* values are negative in the entire sediment column and do not show any distinct vertical trend, with small fluctuation with core depth. Hence, oxidizing conditions are dominant in the entire sediment column at core A1, and the redox condition has not significantly changed. At core A2, the Ce/Ce* values are negative at the top 80 cm and show no anomaly below 80 cm. The sediment column has become the oxidizing condition at the top 80 cm of core A2.

The Eu anomalies represented by Eu/Eu* shows

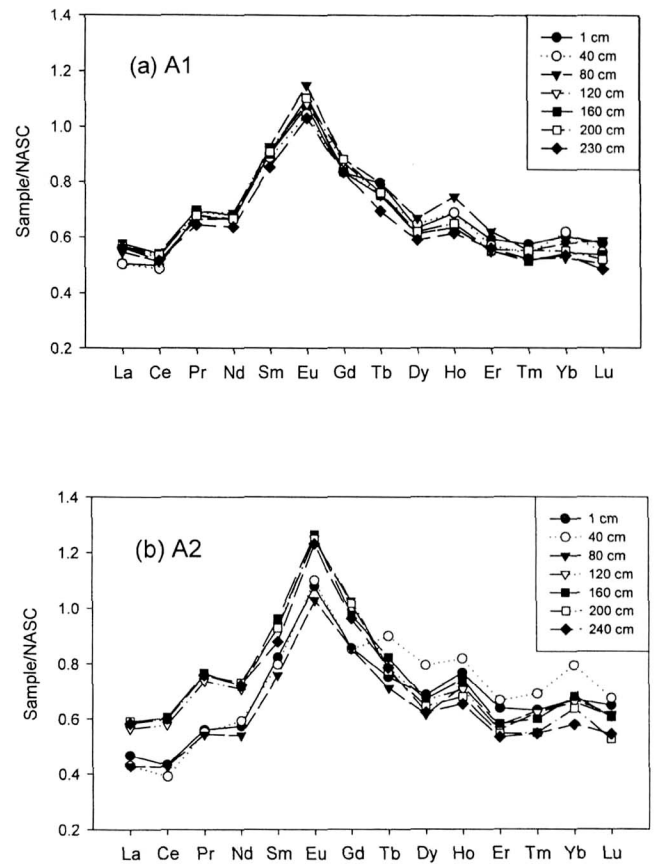

Fig. 7. Shale (NASC)-normalized REE patterns at cores A1 and A2.

positive values in the entire sediment column, without any distinct downcore trend at cores A1 and A2 (Fig. 6c). The positive Eu anomaly is found either in water affected by eolian input or in the hydrothermal solutions and the sediments resulting from high basalt alternation along mid-ocean ridges and back-arc spreading centers (Michard *et al.* 1983; Elderfield

1988). The positive Eu anomalies observed at cores A1 and A2 appear to be affected by the hydrothermal system because the hydrothermal system is located in the center of the Brasfield Strait (Suess *et al.* 1988; Lawver *et al.* 1995).

Shale (NASC)-normalized REE patterns are shown in Fig. 7. At cores A1 and A2, LREEs and HREEs are considerably depleted, but Eu is exclusively enriched in the entire sediment column. The shale-normalized REE patterns in seawater and river water generally show the relative enrichment of LREE and HREE compared to the middle-weight REE (Sm, Eu, Gd, Tb) (Fleet 1984). The shale-normalized REE patterns in seawater and river water are completely opposite to those determined at cores A1 and A2. The shale-normalized REE patterns at cores A1 and A2 are rather similar to those observed in the hydrothermal solutions in which Eu is greatly enriched (McLennan 1989). At cores A1 and A2, therefore, the REE compositions are significantly influenced by the hydrothermal system.

CONCLUSIONS

The major, minor and rare earth elements measured in the Maxwell Bay display different chemical behaviors in the sediment column. Sediment texture, sulfide minerals and $CaCO_3$ are major factors controlling downcore distribution of these elements. The sediment grain size significantly influence the downcore distribution of Ti, Cr, Na, and K at core A1 and Na, Mg, Zn, Cr, Ni, and K at core A2. At both cores, meanwhile, Fe, Co, and Cu concentrations are mainly affected by sulfide minerals.

The rapid increase of La_n/Yb_n values at the boundary of 100 cm core depth of core A1 and A2 indicates that LREEs are fairly depleted at the top 100 cm compared to HREEs. The negative Ce anomalies with no distinct vertical trend at core A1 suggest that oxidizing conditions are dominant in the entire sediment column, and the redox conditions have not significantly changed during the sediment deposition. At core A2, the sediment column has become the oxidizing condition at the top 80 cm. At both cores, the positive Eu anomalies and shale-normalized REE patterns which are similar to those of the hydrothermal solution indicate that the sediments deposited in the Maxwell Bay are significantly influenced by the hydrothermal system.

ACKNOWLEDGMENTS

The sediment cores A1 and A2 were obtained during the tenth cruise of Korea Antarctic Research Program conducted in Korean Ocean Research & Development Institute. The authors thank Drs H-S. Jung and B.K. Khim for their critical reviews of the manuscript.

References

Brookins D.G. 1989. Aqueous geochemistry of rare earth elements. In: Lipin B.P. and McKay G.A. (*eds*), *Geochemistry and Mineralogy of Rare Earth Elements*. Mineralogical Society of America, Washington. pp. 201-226.

Calvert S.E. 1976. The mineralogy and geochemistry of nearshore sediments. *In:* Riley J.P. and Chester R. (*eds*), *Chemical Oceanography*. Academic Press, London. pp. 187-280.

Calvert S.E. and Pedersen T.F. 1993. Geochemistry of recent oxic and anoxic marine sediments: Implications for the geological record. *Mar. Geol.* **113:** 67-88.

Dyrssen D. and Kremling K. 1990. Increasing hydrogen sulfide concentration and trace metal behavior in the anoxic Baltic waters. *Mar. Chem.* **30:** 193-204.

Elderfield H. 1988. The oceanic chemistry of the rare earth elements. *Phil. Trans. Roy. Soc. London* **325:** 105-126.

Elderfield H. and Greaves M.J. 1982. The rare earth elements in seawater. *Nature* **296:** 214-218.

Fleet A.J. 1984. Aqueous and sedimentary geochemistry of the rare earth elements. In: Henderson P. (*ed*), *Rare Earth Element Geochemistry*. Elsevier, Amsterdam. pp. 342-373.

Francois R. 1988. A study on the regulation of the concentrations of some trace metals (Rb, Sr, Zn, Pb, Cu, V, Cr, Ni, Mn and Mo) in Saanich Inlet sediments, British Columbia, Canada. *Mar. Geol.* **83:** 285-308.

Grandjean P., Cappetta H., and Albarede F. 1988. The REE and Nd of 40-70 Ma old fish debris from the west African platform. *Geophys. Res. Lett.* **15:** 389-392.

Hannington M., Herzig P., Scott S., Thompson G., and Rona P. 1991. Comparative mineralogy and geochemistry of gold-bearing sulfide deposits on the mid-ocean ridges. *Mar. Geol.* **101:** 217-248.

Koeppenkastrop D. and De Carlo E.H. 1992. Sorption of rare earth elements from seawater onto synthetic mineral par-

ticles: An experimental approach. *Chem. Geol.* **95:** 251-263.

Lawver A.L., Keller R.A., Fisk M.R., and Strelin J.A. 1995. Bransfield Strait, Antarctic Peninsula active extension behind a dead arc. *In:* Tayler B. (*ed*), *Tectonic and Magmatism*. Plenum Press, New York. pp. 315-342.

Liu Y-G. and Schmitt R.A. 1990. Cerium anomalies in western Indian Ocean Cenozoic carbonates, Leg 115. *Proc. Ocean Drilling Prog. Sci. Res.* **115:** 709-714.

McLennan S.M. 1989. Rare earth elements in sedimentary rocks: Influence of provenance and sedimentary processes. In: Lipin B.P. and McKay G.A. (*eds*), *Geochemistry and Mineralogy of Rare Earth Elements*. Mineralogical Society of America, Washington. pp. 169-200.

Micard A., Albarede F., Michard G., Minister J.F., and Charlou J.L. 1983. Rare earth elements and uranium in high temperature solutions from East-Pacific Rise hydrothermal vent field (13°N). *Nature* **303:** 795-797.

Oudin E. 1985. Trace elements and precious metal concentrations in East Pacific Rise, Cyprus and Red Sea submarine sulfide. In: Teleki P.G., Dobson M.R., Moore J.R., and von Stackelberg U. (*eds*), *Marine Minerals*. NATO ASI Ser. v. 194. pp. 349-362.

Park B-K. and Yoon H.I. 1994. Trace elements in sediments of Admiralty Bay and Bransfield Strait, Antarctica. *Kor. J. Polar Res.* **5:** 13-37.

Piper D.Z. and Isaacs C.M. 1996. Instability of bottom-water redox conditions during accumulation of Quaternary sediment in the Japan Sea. *Paleoceanography* **11:** 171-190.

Pruysers P.A., de Lange G.J., and Middelburg J.J. 1991. Geochemistry of eastern Mediterranean sediments: Primary sediment composition and diagenetic alterations. *Mar. Geol.* **100:** 137-154.

Suess E., Fisk M., and Kadko, D. 1988. Thermal interaction between backarc volcanism and basin sediments in the Bransfield Strait, Antarctica. *Antarctic J. U.S.* **22:** 46-49.

Yoon H.I., Han M.W., Park B-K., Oh J-K., and Chang S-K. 1997. Glaciomarine sedimentation and palaeo-glacial setting of Maxwell Bay and its tributary embayment, Marian Cove, South Shetland Islands, West Antarctica. *Mar. Geol.* **140:** 265-282.

Received 6 July 1999

Accepted 14 September 1999